Polydopamine/poly(sulfobetaine methacrylate) Co-deposition coatings triggered by CuSO$_4$/H$_2$O$_2$ on implants for improved surface hemocompatibility and antibacterial activity

Zhongqiang Zhu [a,1], Qiang Gao [a,1], Ziyue Long [a], Qiuyi Huo [a], Yifan Ge [a], Ntakirutimana Vianney [a], Nishimwe Anodine Daliko [a], Yongchun Meng [b,*], Jia Qu [a,**], Hao Chen [a], Bailiang Wang [a,***]

[a] *School of Ophthalmology & Optometry, Eye Hospital, Wenzhou Medical University, Wenzhou, 325027, China*
[b] *Central Laboratory, Yantai Affiliated Hospital of Binzhou Medical University, 717 Jinbu Street, Yantai, Shandong, 264100, China*

ARTICLE INFO

ABSTRACT

Implanted biomaterials such as medical catheters are prone to be adhered by proteins, platelets and bacteria due to their surface hydrophobicity characteristics, and then induce related infections and thrombosis. Hence, the development of a versatile strategy to endow surfaces with antibacterial and antifouling functions is particularly significant for blood-contacting materials. In this work, CuSO$_4$/H$_2$O$_2$ was used to trigger polydopamine (PDA) and poly-(sulfobetaine methacrylate) (PSBMA) co-deposition process to endow polyurethane (PU) antibacterial and antifouling surface (PU/PDA(Cu)/PSBMA). The zwitterions contained in the PU/PDA(Cu)/PSBMA coating can significantly improve surface wettability to reduce protein adsorption, thereby improving its blood compatibility. In addition, the copper ions released from the metal-phenolic networks (MPNs) imparted them more than 90% antibacterial activity against *E. coli* and *S. aureus*. Notably, PU/PDA(Cu)/PSBMA also exhibits excellent performance *in vivo* mouse catheter-related infections models. Thus, the PU/PDA(Cu)/PSBMA has great application potential for developing multifunctional surface coatings for blood-contacting materials so as to improve antibacterial and anticoagulant properties.

1. Introduction

Medical catheters (such as urinary catheters, intravenous catheters, gastric tubes, etc.) are widely used in clinical practice as implanted biological materials [1–3]. However, due to their materials natural hydrophobicity, these are prone to non-specific proteins adsorption and adhesion/activation of platelets, further leading to clotting and thrombus to cause device failure [4,5]. What's more serious is that bacteria easily adhere to the surface during catheter implantation. Adhering bacteria proliferate rapidly and secrete extracellular matrix (EPS) to form a biofilm [6–8]. To solve these problems, injections of anticoagulants and antibiotics are common clinical treatments. However, drug abuse may cause unavoidable damage to the human body

[9–12]. Hence, endowing the implant materials with good biocompatibility and antibacterial properties are of great clinical significance for its safe and long-term application.

Based on the mechanism of surface-induced thrombosis, various kinds of approaches through surface modification have been explored so as to solve these problems timely and effectively [13]. For instance, hydrophilic polymers (polyethylene glycol (PEG) and its derivatives [14], poly(vinyl pyrrolidone) (PVP) [15,16], etc.) and anticoagulant agents (heparin, bivalirudin etc.) are often used for building anti-coagulation surfaces [17,18]. Although these approaches have been widely used in research, there are still major limitations in practical applications because most of the available ones usually involve complex procedures and have poor blood compatibility. Especially, zwitterionic

polymers, such as poly-(sulfobetaine methacrylate) (PSBMA), poly-(-carboxybetaine methacrylate) (PCBMA), poly (2-methacry-loyloxyethyl phosphorylcholine) (PMPC), have been extensively used for surface modification of all kinds of medical devices due to their excellent hydrophilic, nonfouling, and biocompatibility properties [19–21]. It has been hypothesized that, with both positively and negatively charged moieties, the zwitterionic polymers can strongly bind water molecules via electrostatically induced hydration, so they exhibit high resistance against nonspecific protein adsorption and also efficiently avoid bacterial adhesion to prevent formation of long-term bacterial biofilm [22–24]. Hence, zwitterionic polymers have been an ideal candidate for construction of biomaterials with good blood compatibility.

The development of bacteria is another important problem that greatly threats the using of implants. Injecting antibiotics for several days after implanting the medical device is a common way. However, the abuse of antibiotics in medical treatment has led to an increase in the prevalence of resistant bacteria [25]. Therefore, to prevent the occurrence of device-associated infection, more effective method is to modify the bactericidal chemicals on the surface of the material [26]. Currently, the commonly used antibacterial agents are metal nanoparticles [27], metal ions [28,29], quaternary ammonium salts [30], antimicrobial peptides and polymer [31], etc. As an essential trace element in the human body, copper is one of the earliest inorganic antibacterial agents used by human. In 2500 BC, the Egyptians had used copper to clean their wounds. Copper also had been widely used for treatment of wound infection and other diseases before the discovery of antibiotics [32]. According to previous reports, the high concentration of copper ions outside will cause the difference in the concentration of ions inside and outside the cell membrane, which will destroy the transportation of nutrients (Na^+/K^+, glutamate, etc.) required by the cell and cause its death. In addition, copper ions could bind to bacterial surface and destroy the cell membrane, inducing leakage of intracellular components and causing cell death. Therefore, the excellent antibacterial property of copper ion could prompt us to choose it as a surface decoration agent to construct antibacterial biomaterials [33].

Based on the above description, we know that the construction of a material with both antibacterial and anticoagulant is of great significance in clinical applications. Although the emerging applications of nitric oxide release have been extensively studied in overcoming antithrombotic and anti-bacterial medical devices, there are still problems such as short lifetime and poor blood compatibility [34–39]. In contrast, the use of copper ions and zwitterionic polymers to modify implant materials has unparalleled advantages. However, it is still a challenge to solve how to anchor zwitterionic polymers and metal ions on the surface with ease. Bio-inspired polydopamine (PDA) has been regarded as a universal and versatile platform for simple surface modification of
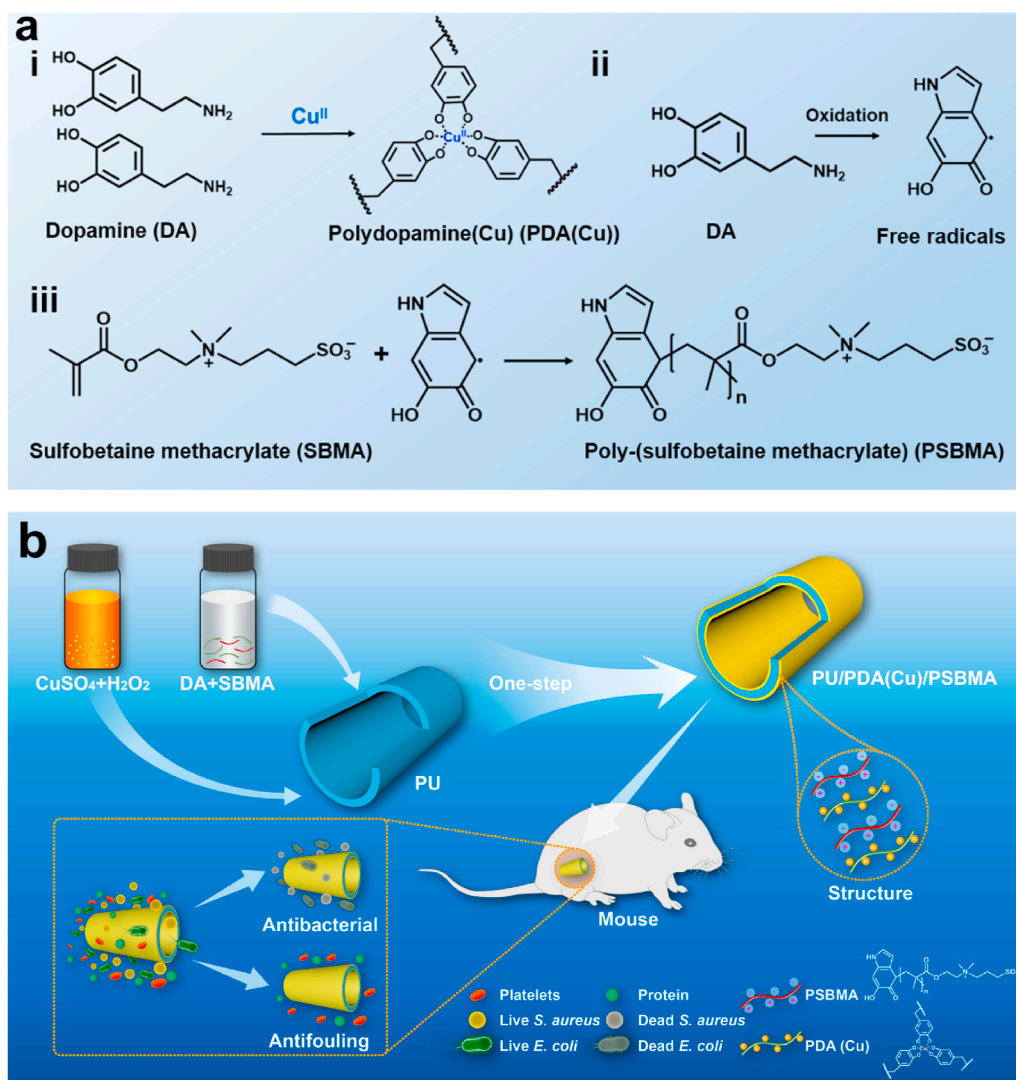
Scheme 1. Schematic of the preparation of the PU/PDA(Cu)/PSBMA. (a) (i) The chemical structure of PDA and copper ion forming MPNs. (ii, iii) The mechanism of the DA-triggered polymerization of SBMA. (b) PU/PDA(Cu)/PSBMA exhibits both antibacterial and antifouling properties.

medical devices, but the main drawbacks of state-of-the-art PDA coatings lie in the low efficiency and poor stability [40,41]. Most recently, Xu et al. proposed that CuSO$_4$/H$_2$O$_2$ is able to notably accelerate the co-deposition process of PDA with PSBMA [42]. During the polymerization of dopamine (DA), Cu^{2+} and H$_2$O$_2$ produce reactive oxygen species (ROS), such as O$_2^{\cdot-}$, OH$_2^{\bullet}$ and OH$^{\bullet}$ in alkaline medium. These free radicals could accelerate the oxidation and polymerization of DA in the solution, thus improving the deposition efficiency with PSBMA [43]. In this study, CuSO$_4$/H$_2$O$_2$ was used to trigger PDA and PSBMA co-deposition process to endow polyurethane (PU) antibacterial and antifouling surface (PU/PDA(Cu)/PSBMA) (Scheme 1). The constructed PDA coating contains copper ions and catechol groups to form metal-phenolic networks (MPNs) to endow the surface with good stability and antibacterial properties [44–46]. In addition, PDA can also act as an initiator to induce the polymerization of sulfobetaine methacrylate (SBMA) monomer and can be anchored on the surface of the substrate for good antifouling performance. Then we comprehensively evaluated the blood compatibility, protein/platelet resistance, cytotoxicity and anti-infective properties of these materials *in vitro* and *in vivo,* the results indicated the materials that we constructed have promising prospect for being used as excellent implanted biomaterials.

2. Experiment section

2.1. Materials

Dopamine hydrochloride and SBMA were purchased from Sigma-Aldrich (USA). Copper (II) sulfate pentahydrate (CuSO$_4$·5H$_2$O, 99%), hydrogen peroxide (H$_2$O$_2$, 30%), tris (hydroxymethyl) aminomethane (Tris) were obtained from Aladdin (China), respectively. Dulbecco's modified Eagle Medium (DMEM) and fetal bovine serum (FBS) were purchased from Gibco Life Technologies (USA). Fluorescently-labeled bovine serum albumin (FL-BSA), BSA and Fg regents were obtained from Bioss Biotech (China). LIVE/DEAD Viability/Cytotoxicity kit (L3224), LIVE/DEAD BacLight bacterial viability kit (L7012) and Cell Counting Kit-8 (CCK-8) were purchased from Thermo Fisher (USA). *S. aureus* (ATCC6538) and *E. coli* (ATCC 8739) were kindly provided by Prof. Jian Ji (Zhejiang University). Ultrapure water was obtained from a Milli-Q system (Millipore, USA). All the other chemical reagents, unless mentioned, were purchased from Aladdin (China).

2.2. Preparation of PU/PDA(Cu)/PSBMA

First, DA and SBMA monomer were all dissolved in Tris buffer solution (50 mM, pH 8.5). Then, CuSO$_4$·5H$_2$O (5 mM, 62.5 mg) and H$_2$O$_2$ (19.6 mM, 0.1 mL) were dosed sequentially. The concentration of DA was kept at 2 mg/mL, and the mass ratio of DA/SBMA was 1:15. PU samples were first pre-wetted by ethanol and then immersed in the above solutions in an air oscillator at room temperature for 4 h. After that, the samples were washed by deionized water and dried at 55 °C for 4 h. In this study, the single DA coating (PU/PDA), a DA coating with copper ions (PU/PDA(Cu)) and a DA/SBMA coating(PU/PDA/PSBMA) were also prepared on the PU surface using the same method as the control.

2.3. Characterization

^{1}H NMR spectra (Bruker DMX500, 500 Hz, USA) was employed to prove the successful synthesis of PSBMA copolymer. A field-emission scanning electron microscope (SEM, Hitachi SU8000, Japan) was used for characterizing the surface morphologies of the samples. The surface chemical compositions of the samples was measured by X-ray photo-electron spectrometer (XPS, PerkinElmer, USA), and the hydrophilicity and thickness of the coatings by water contact angle analysis (Biolin, Theta, Sweden) and spectroscopic ellipsometry (J. A. Woollam, M-2000UI, USA), respectively, and the UV–vis absorption of the solutions

by an ultraviolet spectro-photometer (Agilent, CARY5000, USA).

2.4. Evaluation of coatings stability

In order to evaluate the stability of the surface coating, PU/PDA(Cu)/PSBMA was immersed in 2 mL of PBS (pH 5.5, pH 7.4, pH.8.5, respectively) and shaken at 120 rpm under 37 °C for 7 days. A quantitative solution was taken on day 1, day 3, and day 7, and the absorbance of the solution at 420 nm was measured by ultraviolet spectro-photometer. Moreover, the structure stability of this PU/PDA(Cu)/PSBMA was also investigated by monitoring the thickness change of the coating.

2.5. In vitro antibacterial property

The antibacterial properties of materials modified by different methods were tested according to the previous reported method [38,47]. Briefly, the samples after high temperature sterilization were first placed in a 24-well plate, and then 200 μL of bacteria (*E. coli* or *S. aureus*) suspension that was diluted to 1.0 × 10^6 CFU/mL was added. After incubation in shaker at 37 °C for 24 h, the bacteria in the suspension were inoculated on Luria-Bertani (LB) agar plates with 10-fold serial dilutions for counting. Finally, the relative bacterial survival rate was calculated based on the number of colonies. In addition, LIVE/DEAD staining was performed to explore the survival and adhesion ability of bacteria in contact with these surfaces.

2.6. In vitro anti-adhesion of bacteria activity

The anti-adhesion of bacteria activity of the samples was evaluated against bacteria of *E. coli* and *S. aureus*. Briefly, fresh bacteria suspension (2 mL, 1 × 10^8 CFU/mL) was cultured with different samples in 24-well culture plate and incubated for 24 h at 37 °C. Next, removed the planktonic bacteria and washed three times with sterile PBS buffer solution. Subsequently, 2.5% glutaraldehyde was used for fixing the samples overnight followed by ethanol gradient dehydration (25, 50, 75 and 100 wt%, respectively) for 10 min in each step. Finally, the obtained samples were dried for SEM observation.

2.7. Protein adsorption assay

BSA and Fg were selected as model proteins to evaluate the protein adsorption analysis of different samples. Briefly, all samples were immersed in PBS buffer solution in a 96-well plate overnight and then separately submersed in protein solution (2 mg/mL, 200 μL) and incubated at 37 °C for 4 h. Next, all samples were washed 3 times with deionized water to remove unabsorbed proteins. Finally, all samples were sonicated in sodium dodecyl sulfate (SDS) (2 wt %, 200 μL) solution for 1 h to detach the proteins adsorbed on the surface, and the supernatant (100 μL) from each well was placed in a new 96-well, supplementing with 100 μL of BCA working solution to test the absorbance at 560 nm by the microplate reader (Varioskan LUX, Thermo Fisher). Additionally, all samples treated with FL-BSA were used for qualitative observation of adsorption status of BSA on the surface by fluorescence microscope (Zeiss, Germany).

2.8. Hemolysis test

Red blood cells (RBCs) were separated from the rabbit blood and seeded in 2 mL centrifuge tube, and all samples dispersed in NaCl solution then were incubated with RBCs under shaking culture at 37 °C for 2 h. For comparison, RBCs treated with equal volume of deionized water and NaCl solution were used as positive and negative control groups, respectively. After all samples were centrifuged for 10 min at 3000 rpm to obtain supernatant liquid, the absorbance at 545 nm was measured with a microplate reader. The hemolysis ratio was obtained in accordance with following equation (OD$_{pos}$ and OD$_{neg}$ are the absorbance of

positive and negative control groups at 545 nm, respectively):

$$Hemolysis\ ratio\ (\%) = \frac{OD_{test} - OD_{neg}}{OD_{pos} - OD_{neg}} \times 100\%$$

2.9. Platelet adhesion

Fresh citrated whole blood was centrifuged for 10 min at 1000 rpm to obtain platelet-rich plasma (PRP). All samples were balanced in PBS of pH 7.4 for 12 h and then separately submersed in 200 μL of PRP and incubated at 37 °C for 2 h. All surfaces were cleaned softly with PBS three times and fixed with 2.5% glutaraldehyde for 4 h at room temperature. Finally, samples were dehydrated through a series of graded ethanol-water solutions (25, 50, 75 and 100 wt %, each for 15 min) and then were dried and gold-coated.

2.10. In vitro cytotoxicity assay

The CCK-8 and Live/Dead cell staining kit assay were applied to assess the compatibility of the samples with HUVECs. Briefly, HUVECs were initially harvested and seeded into 24-well plate for 12 h for attachment (1×10^4 cells/well), and then sterilized samples were seeded onto tissue culture plate containing fresh medium, and incubated in a humidified incubator at 37 °C/5% CO_2 for 2 h, 24 h and 48 h, respectively. After that, the previous samples were carefully removed by sterile forceps from the culture medium, the cells were washed 3 times with PBS and then CCK-8 reagent (10% in DMEM media) or Calcein-AM/PI dual staining solution was added to 24-well plate. The absorbance at 450 nm was measured by Microplate Reader, and Live/Dead cell staining was observed with an inverted fluorescence microscope.

2.11. In vivo antibacterial assay

All the animal procedures were performed in compliance with the guidelines of the Institutional Animal Care and Use Committee of Wenzhou Medical University (Wenzhou, China). The experiment used approximately 0.4 kg Sprague Dawley (SD) rats obtained from the Animal Management Center of Wenzhou Medical University. The animal models were based on our previous experimental methods. Briefly, catheters were cut into segments, with then immediately implanted into the back of the SD rats that were anesthetized. The wounds healing of the catheters implantation site in SD rats was observed on day 1, day 3 and day 7. After the rats were euthanized, the implanted catheter samples were taken out on day 7. The bacteria adsorbed on the surface of catheters were dispersed in the PBS buffer solution by ultrasound, and then we counted the survival status of the bacteria as per the previous method. The surrounding skin was cut off, fixed, dehydrated and embedded in paraffin, and then sectioned for hematoxylin and eosin (H&E) staining and observation.

2.12. Statistical analysis

All data were obtained from at least three replicate experiments and expressed as the mean ± standard deviation. Statistical significance was evaluated by means of the two-tailed Student's *t*-test between different groups. The difference of *$p < 0.05$ is statistically significant under consideration.
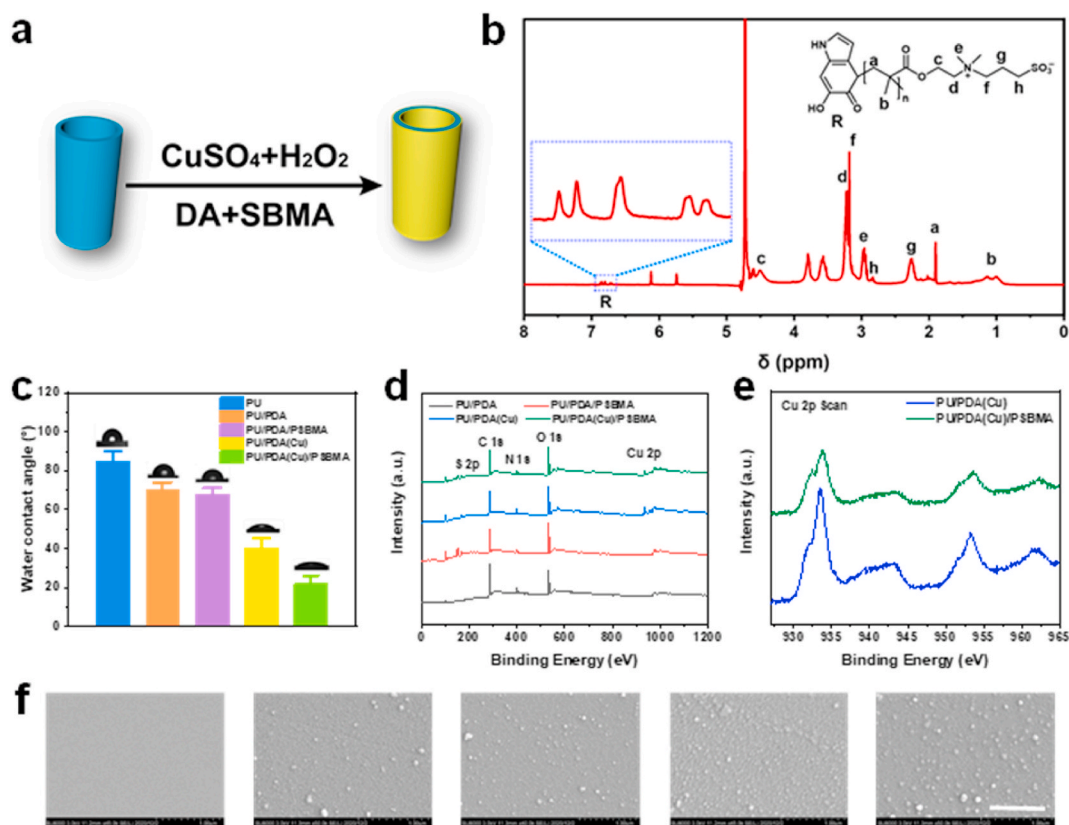

Fig. 1. (a) Schematic illustration of the preparation of PU/PDA(Cu)/PSBMA. (b) ^{1}H NMR spectra of PSBMA in D_2O. (c) Contact angle measurement of the PU/PDA, PU/PDA/PSBMA, PU/PDA(Cu) and PU/PDA(Cu)/PSBMA coating. (d) XPS of the PU/PDA, PU/PDA/PSBMA, PU/PDA(Cu) and PU/PDA(Cu)/PSBMA coating. (e) High Cu 2p scan of the PU/PDA(Cu)/PSBMA coating. (f) SEM images of the PU, PU/PDA, PU/PDA/PSBMA, PU/PDA(Cu) and PU/PDA(Cu)/PSBMA coating. Scale bar: 1 μm.

3. Results and discussion

3.1. Preparation and characterization of the PU/PDA(Cu)/PSBMA

Herein, a novel coating based on the co-deposition of PDA and PSBMA triggered by $CuSO_4/H_2O_2$ was simply prepared onto the surface of PU (PU/PDA(Cu)/PSBMA) (Fig. 1a). In this study, PDA acted as both the polymerization initiator and the adhesive sites. First, in order to prove that DA could induce the polymerization of SBMA monomer, the structure of the polymerized product was characterized by ^{1}H NMR. As shown in Fig. 1b, the chemical potential peaks in the ^{1}H NMR date were 4.50, 3.77, 3.52, 3.14, 2.94, 2.19, 2.97, and 1.00–1.29 ppm in sequence. The comparison showed that they belonged to the proton peaks in PSBMA. In addition, a proton peak appeared at the position of 3.59 ppm chemical shift, which was a unique peak of Tris, indicating that Tris was also involved in the reaction. The proton peak also appeared at the chemical shift position of 6.6–7.0 ppm in the spectrum, which proved that DA also participated in the above reaction and was retained in PSBMA. In addition, we monitored the UV–Vis absorbance changes of various DA solutions at 420 nm (Fig. S1). The absorbance of the solution with $CuSO_4/H_2O_2$ also increased to more than 3.0, which was much higher than that of DA (1.6) and DA (0.82) with SBMA. Fig. S2 shows that the color of the pristine PU catheter was changed from white to PDA-like light grey, indicating successful formation of the coating.

Next, the thickness of these PU films modified by different methods was measured. As seen in Fig. S3, the thickness of PU/PDA and PU/PDA/PSBMA coatings was less than 10 nm after 4 h, while the thickness of PU/PDA(Cu) and PU/PDA(Cu)/PSBMA reached 30 nm. Therefore, the polymerization of DA and the deposition rate of PDA coating were greatly accelerated and triggered by $CuSO_4/H_2O_2$. Similarly, the contact angle decreased from $85 \pm 5°$ to $22 \pm 4°$ (Fig. 1c), which became more hydrophilic after incorporation of PSBMA. The increase of thickness makes the surface of the coating contain more copper ions and zwitterions, which endows the surface with antibacterial and hydrophilic properties, and good hydrophilicity to effectively inhibit the adsorption of bacteria, platelets and non-specific proteins on the surface [48,49].

The XPS analysis was performed on the surface chemical composition of these samples for further confirmation of successful decoration. As shown in Fig. 1d and e, the Cu 2p peak at 935.0 eV was observed in the PU/PDA(Cu) and PU/PDA(Cu)/PSBMA, that demonstrated the formation of MPNs. Additionally, the spectra for PU/PDA/PSBMA and PU/PDA(Cu)/PSBMA, a strong S 2p peak at 170.0 eV and the N 1s peak at 402.2 eV were shown, which corresponded to the C–N$^+$ bonds and S element of the PSBMA (and S4) respectively. Notably, the spectrum showed that all samples also had an N 1s peak at 399.0 eV, which was attributed to the C–N bond of PDA. Further, changes in surface morphology of the PU were observed by SEM. According to Fig. 1f, the original surface exhibited smooth surface topography, while surface modification led to rough surface morphology. Moreover, the surface roughness of PU/PDA(Cu)/PSBMA significantly increased, which showed that the surface modification reactions went on smoothly on material surface.

3.2. Stability of PU/PDA(Cu)/PSBMA coatings

Coating stability is an important indicator for the safety of implant materials. To investigate its stability, the silicon wafer modified by the same method was immersed in different PBS buffer solutions (pH = 5.5, 7.2 and 8.5), and the thickness of the coating was monitored. As shown in Fig. 2a–c, after all samples were soaked in PBS buffer solutions with pH = 7.2 and pH = 8.5 for 7 days, respectively, the coating thickness was reduced by about 10%, even in the acidic buffer solution with pH = 5.5, the coating thickness was only reduced by about 20%. Furthermore, UV–Vis spectroscopy was used to detect the PDA content in the solution
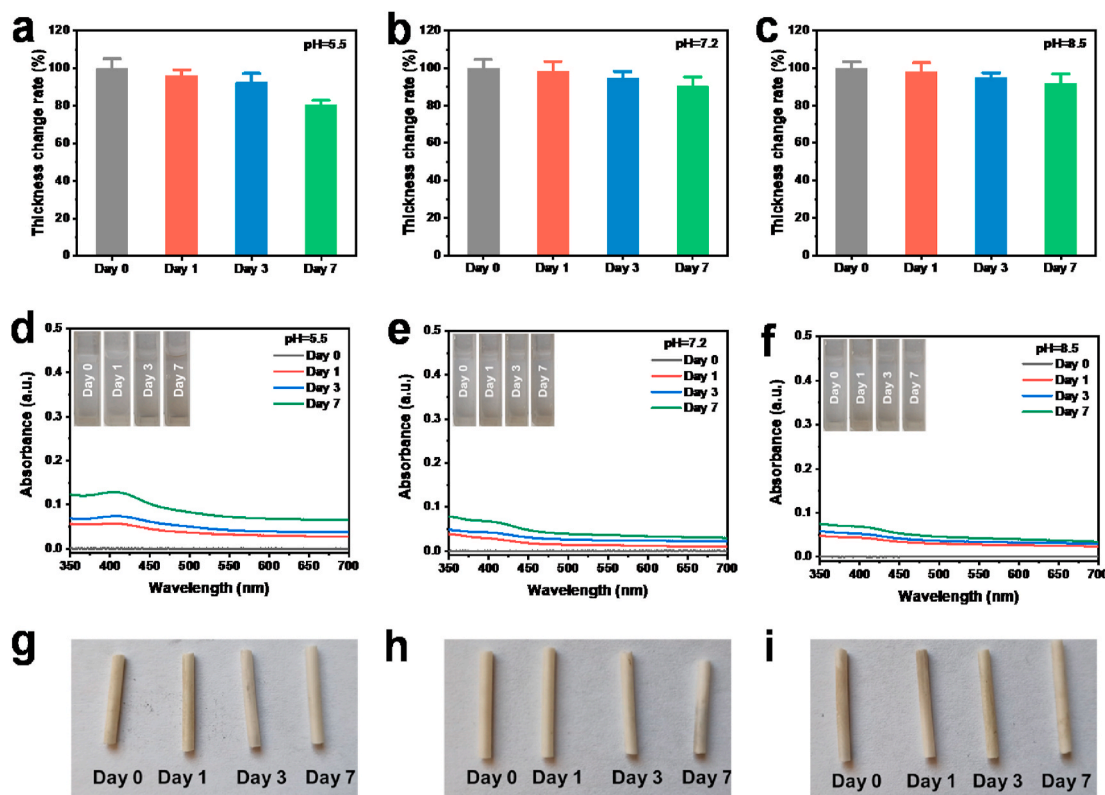

Fig. 2. Thickness change rate of PU/PDA(Cu)/PSBMA immersed in different PBS buffer solutions ((a) pH = 5.5, (b) pH = 7.2, (c) pH = 8.5) on day 0, 1, 3 and 7. UV–vis spectra of different eluents ((d) pH = 5.5, (e) pH = 7.2, (f) pH = 8.5) of PU/PDA(Cu)/PSBMA on day 0, 1, 3 and 7. Photographs of PU/PDA(Cu)/PSBMA catheters immersed in different PBS buffer solutions ((g) pH = 5.5, (h) pH = 7.2, (i) pH = 8.5) on day 0, 1, 3 and 7.

and the color change of the catheter also showed similar results (Fig. 2d–i). The elemental composition of the surface was the same as the initial state, and the morphology and water contact angle almost unchanged (Figs. S5–S7). These results indicated the good stability of the coating which was suitable for long-term use in the human body. The good stability of the PU/PDA(Cu)/PSBMA coating may benefit from such reason that the residual copper ions could act as cross-link sites by chelation with the amine and imine groups of PDA, which is the same as the mechanism reported in the literature that iron ions can enhance the stability of the PDA coating [50,51].

3.3. Anti-protein adsorption and hemocompatibility

According to the mechanism of thrombus formation, the adsorption of non-specific proteins on the surface has an important influence on thrombus formation, and the construction of a biomaterial surface with low protein adsorption was a solution [5]. Fg and BSA are key proteins in the coagulation cascade, and play a leading role in mediating the adhesion and activation of platelets to the surface of the material [52, 53]. Therefore, we choose Fg and BSA as model proteins to evaluate the protein adsorption capacity of different samples. As shown in Fig. 3a and b, when the PU surface modified by PDA or PSBMA is used alone, due to the slow polymerization of DA, even if the successful modification of PSBMA is detected, the PSBMA coating cannot cover it completely, so it

may cause PU/PDA/PSBMA to have lower anti-protein adsorption capabilities. However, when CuSO₄/H₂O₂ is added, the polymerization of DA and SBMA were accelerated, leading to the formation of a large number of hydrophilic groups on the surface of PU, so that PU/PDA(Cu) and PU/PDA(Cu)/PSBMA exhibits good anti-protein adsorption ability. Especially for PU/PDA(Cu)/PSBMA surface, the protein adsorption of Fg and BSA was even reduced by 70% and 88%. In addition, we also observed the adsorption of FL-BSA on the surface of different samples through a fluorescence microscope (Fig. 3c). It can be seen that the surfaces of PU, PU/PDA, PU/PDA/PSBMA and PU/PDA(Cu) showed strong fluorescence, while PU/PDA(Cu)/PSBMA almost undetectable fluorescence, showing the excellent anti-protein adsorption performance of PU/PDA(Cu)/PSBMA.

The adhesion and activation of platelets is another important cause of thrombus formation [54]. When Fg and other adhesive proteins adhere to the surface of the material, they interact with the receptors on the platelet surface to regulate the adhesion and activation of platelets, and the activated platelets will secrete and release adenosine diphosphate (ADP), thromboxane A2 (TXA2) and other substances. These substances in turn regulate the binding of Fg and other viscous proteins to platelets and accelerate platelet aggregation, and form a cascade reaction that ultimately leads to the formation of thrombus [55]. Therefore, a good blood contact material must be able to effectively inhibit the adhesion of platelets, and the following experimental results just prove
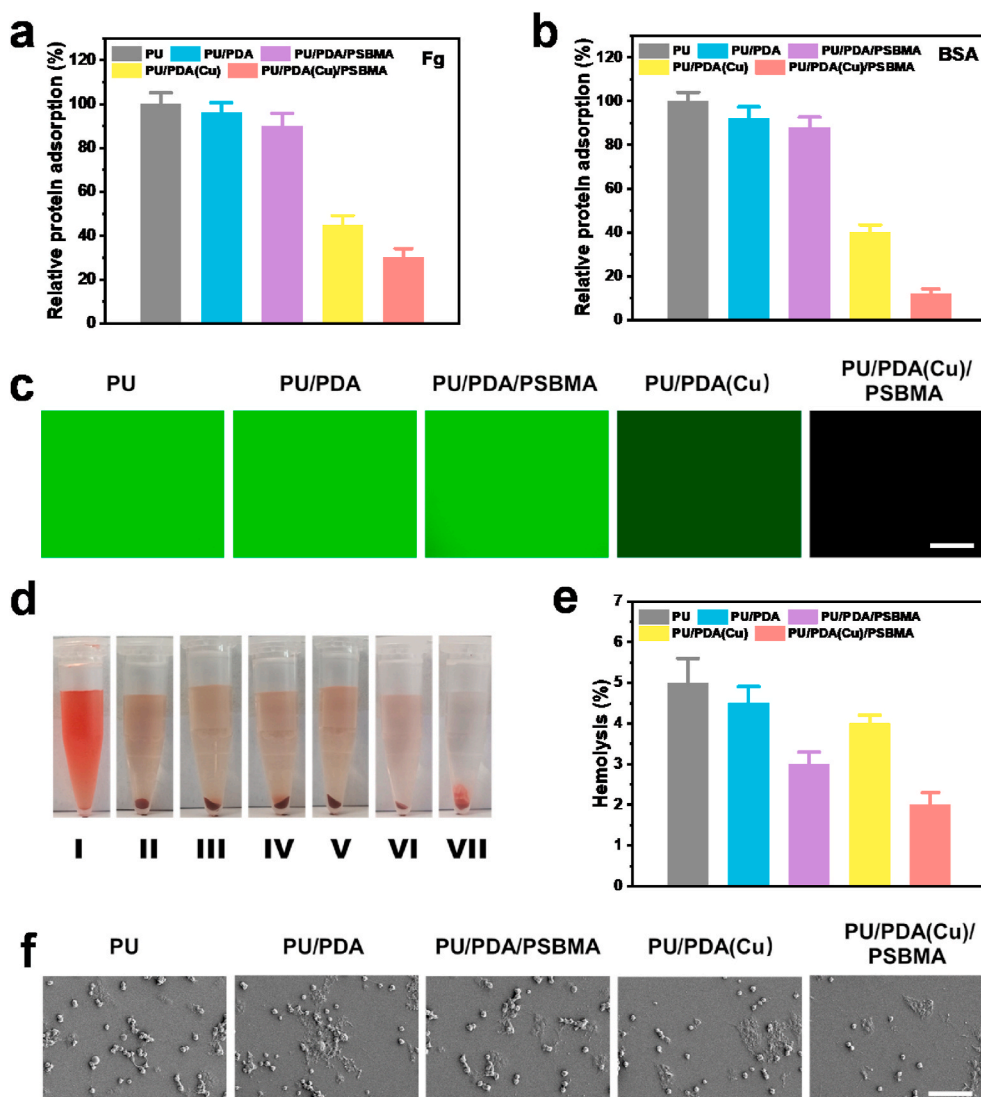

Fig. 3. Relative protein adsorption (a) Fg and (b) BSA on the surface of PU, PU/PDA, PU/PDA/PSBMA, PU/PDA(Cu) and PU/PDA(Cu)/PSBMA. (c) Fluorescence microscopy images of FL-BSA adsorption on the surface of PU, PU/PDA, PU/PDA/PSBMA, PU/PDA(Cu) and PU/PDA(Cu)/PSBMA. Scale bar: 20 μm. (d) Images of hemolysis analysis of positive control (I), PU (II), PU/PDA (III), PU/PDA/PSBMA (IV), PU/PDA(Cu) (V), PU/PDA(Cu)/PSBMA (VI) and negative control (VII). (e) Hemolysis rate of PU, PU/PDA, PU/PDA/PSBMA, PU/PDA(Cu) and PU/PDA(Cu)/PSBMA. (f) Platelet adhesion on the PU, PU/PDA, PU/PDA/PSBMA, PU/PDA(Cu) and PU/PDA(Cu)/PSBMA surfaces observed with SEM. Scale bar: 20 μm.

this point. As shown in Fig. 3f and S8, a large number of activated platelets (2.74×10^4 platelets/mm^2) adhered to the unmodified PU surface. In contrast, the density of platelets adhered to the modified PU surface was lower, especially the density on surface of PU/PDA (Cu)/PSBMA was only 0.54×10^4 platelets/mm^2, which was about 19.7% of that on the unmodified PU surface. Besides, the hemolysis rate of all samples was lower than 5% (Fig. 3d and e), which also proved the substrate with good blood compatibility.

3.4. In vitro antibacterial property assay

Infection caused by bacteria is one of the main complications of implant materials. Surface modification with antibacterial agents is a good choice to endow these devices with potent antibacterial [56]. To illustrate the antibacterial property of modified PU materials, *E. coli* and *S. aureus* were chosen for antibacterial characterization. As shown in Fig. 4a, the number of colonies of the two bacteria decreased significantly after incubating with PU/PDA(Cu) and PU/PDA(Cu)/PSBMA surfaces, while no obvious change in colonies count change was observed in other modified PU materials compared to pristine PU film. According to quantitative analysis, there was a marked reduction up to 2 log by the coating containing copper ions against both *S. aureus* and *E. coli* bacteria (Fig. 4b and S9). The bactericidal and anti-adhesive activities of the all samples were explored through bacterial LIVE/DEAD staining method and SEM measurement. As shown in Fig. 4c, intense green fluorescence was observed in the groups of pristine PU, PU/PDA and PU/PDA/PSBMA surface for both *E. coli* and *S. aureus* bacterial, indicating that a large number of live bacteria adhered to the surface of the material. The PU/PDA(Cu) and PU/PDA(Cu)/PSBMA surface however showed a significant reduction in the adhered bacteria. By contrast, the excellent anti-fouling and antibacterial activities were exhibited since just a few of dead bacteria adhered to the surface.

To further verify the bacterial anti-adhesion function, SEM images were obtained to distinguish the remaining bacteria from bacterial corpse on different samples. As shown in Fig. 5a and b, a lot of bacteria with normal and intact cell membranes adhered to the surface of the pristine PU, PU/PDA and PU/PDA/PSBMA. However, the cell membranes of the attached bacteria in the other two groups were partially destroyed and the cytoplasm leaked. Especially, only a small amount of bacteria adhered to the surface of PU/PDA(Cu)/PSBMA. According to the quantitative analysis, the densities of the two bacteria adhering to

the PU/PDA(Cu)/PSBMA surface reduced about 90% compared with the unmodified PU surface (Fig. 5c and d), which suggested the antiadhesive and antibacterial properties of modified PU. In addition, it was also noticed that PU/PDA(Cu)/PSBMA exhibited different antibacterial properties against *E. coli* and *S. aureus*. The reason may be that the cell wall structure of Gram-positive are different from that of Gram-negative bacteria, which led to the different antibacterial characteristics of the coatings [57,58].

3.5. In vitro biocompatibility evaluation

To further evaluate the *in vitro* cytotoxicity, the HUVECs on the surface of the 24-well plate were incubated with different samples and then subjected to Live/Dead staining and CCK-8 test. As shown in Fig. S10, 6a and 6c, the fluorescence images showed that after incubating HUVECs with all samples for 2 h, 24 h and 48 h respectively, except for a few dead cells on the surface of PU/PDA(Cu) and PU/PDA (Cu)/PSBMA, little dead cells appeared in other groups, showing negligible cytotoxicity. In addition, this result was also verified by CCK-8 test. After 48 h of incubation with HUVECs, the absorbance of all samples at 450 nm increased significantly (Fig. 6b and d), indicating that they all had excellent cell proliferation ability and biocompatibility.

3.6. In vivo evaluation

According to above study, the surface of PU/PDA(Cu)/PSBMA exhibited excellent properties such as antibacterial, anti-adhesion and protein/platelet-resistance in *vitro*, but these properties may be destroyed or even failed when entering the body. Therefore, we established an animal model related to the catheter-induced infection to evaluate its properties *in vivo*. We initially cut a wound with an average size of about 1.5 cm on the back of the mouse, and then different samples contaminated with *S. aureus* were immediately implanted. As seen in Fig. 7a, there was no significant difference in the external wounds among all the groups on day 1 after implantation. After the day 7 of implantation, the wounds between all groups were basically healed and there was no significant difference. In addition, we cut and opened the infected skin to explore the appearance of inflammation inside. A large amount of white pus was detected in the group implanted with PU, PU/ PDA and PU/PDA/PSBMA, which indicated a severe inflammatory response due to bacterial infection. In contrast, the minimal infection
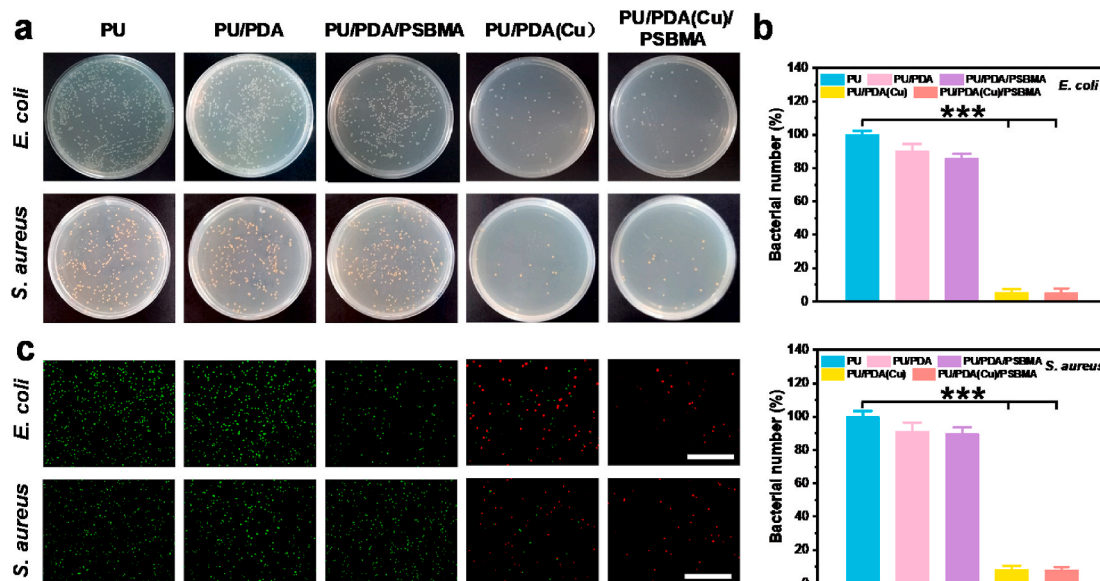

Fig. 4. (a) Agar plate photographs, (b) relative bacterial numbers and (c) live/dead assay of *E. coli* and *S. aureus* after incubation with PU, PU/PDA, PU/PDA/PSBMA, PU/PDA(Cu) and PU/PDA(Cu)/PSBMA, respectively. Scale bar: 20 μm. (***$P < 0.001$).
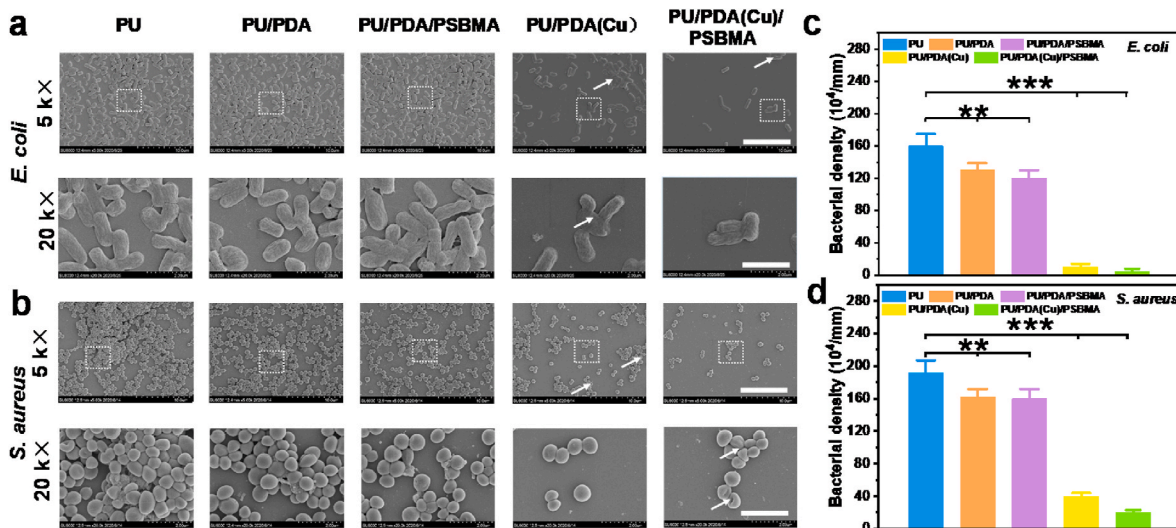
Fig. 5. SEM images showing the anti-adhesive properties of PU, PU/PDA, PU/PDA/PSBMA, PU/PDA(Cu) and PU/PDA(Cu)/PSBMA in the presence of (a) *E. coli* and (b) *S. aureus* at different magnifications (upper panel, 5 k, Scale bar: 10 μm; lower panel, 20 k, Scale bar: 2 μm) (the white arrow indicates dead bacteria). Bacterial density adhering to the surface of PU, PU/PDA, PU/PDA/PSBMA, PU/PDA(Cu) and PU/PDA(Cu)/PSBMA in the presence of (c) *E. coli* and (d) *S. aureus* (**$p < 0.01$, ***$p < 0.001$).
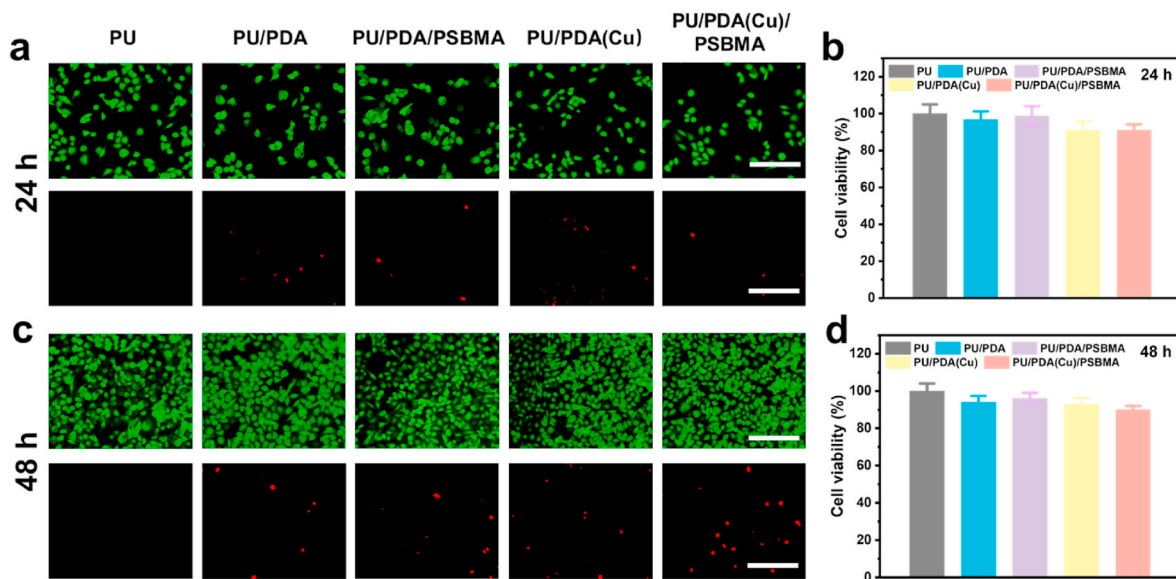

Fig. 6. (a) Fluorescent images of LIVE/DEAD staining (b) cell viability on HUVECs after incubation with PU, PU/PDA, PU/PDA/PSBMA, PU/PDA(Cu) and PU/PDA (Cu)/PSBMA for 24 h. (c) Fluorescent images of LIVE/DEAD staining (d) cell viability on HUVECs after incubation with PU, PU/PDA, PU/PDA/PSBMA, PU/PDA(Cu) and PU/PDA(Cu)/PSBMA for 48 h. Scale bar: 20 μm.

was shown in other two groups due to little secretion. We also evaluated the concentration of bacteria adhering to the surface of the catheter and observed the tissue slices around the wound. As shown in Fig. 7b and S11, the bacterial concentration of PU/PDA(Cu) and PU/PDA(Cu)/PSBMA groups was reduced by 70% compared with the other three control groups, indicating excellent bacteria-killing properties in the group containing copper ions. According to H&E staining images, many inflammatory cell infiltrations were observed in the pristine PU, PU/PDA and PU/PDA/PSBMA groups (Fig. 7c). On the contrary, the above pathological changes were alleviated in the other two groups.

4. Conclusion

In summary, we presented a rapid, simply and one-step strategy to fabricate functionalized surfaces of PU via the CuSO$_4$/H$_2$O$_2$-triggered

co-deposition of PDA and PSBMA. This method not only endows the surface of PU/PDA(Cu)/PSBMA with excellent biocompatibility, blood compatibility, bactericidal and anti-adhesion activities *in vitro*, but also significantly improves the deposition efficiency and stability compared with traditional methods. More importantly, the excellent performance of PU/PDA(Cu)/PSBMA is still maintained *in vivo* mice models, which can successfully inhibit the growth of bacteria and prevent catheter-related infections caused by *S. aureus*. This work provides a simple and effective method for addressing the major clinical complications of blood-contacting biomaterials and medical devices.

Author contributions

All of the authors participate in the experiments or writing work. Zhongqiang Zhu completed surface modification and wrote the
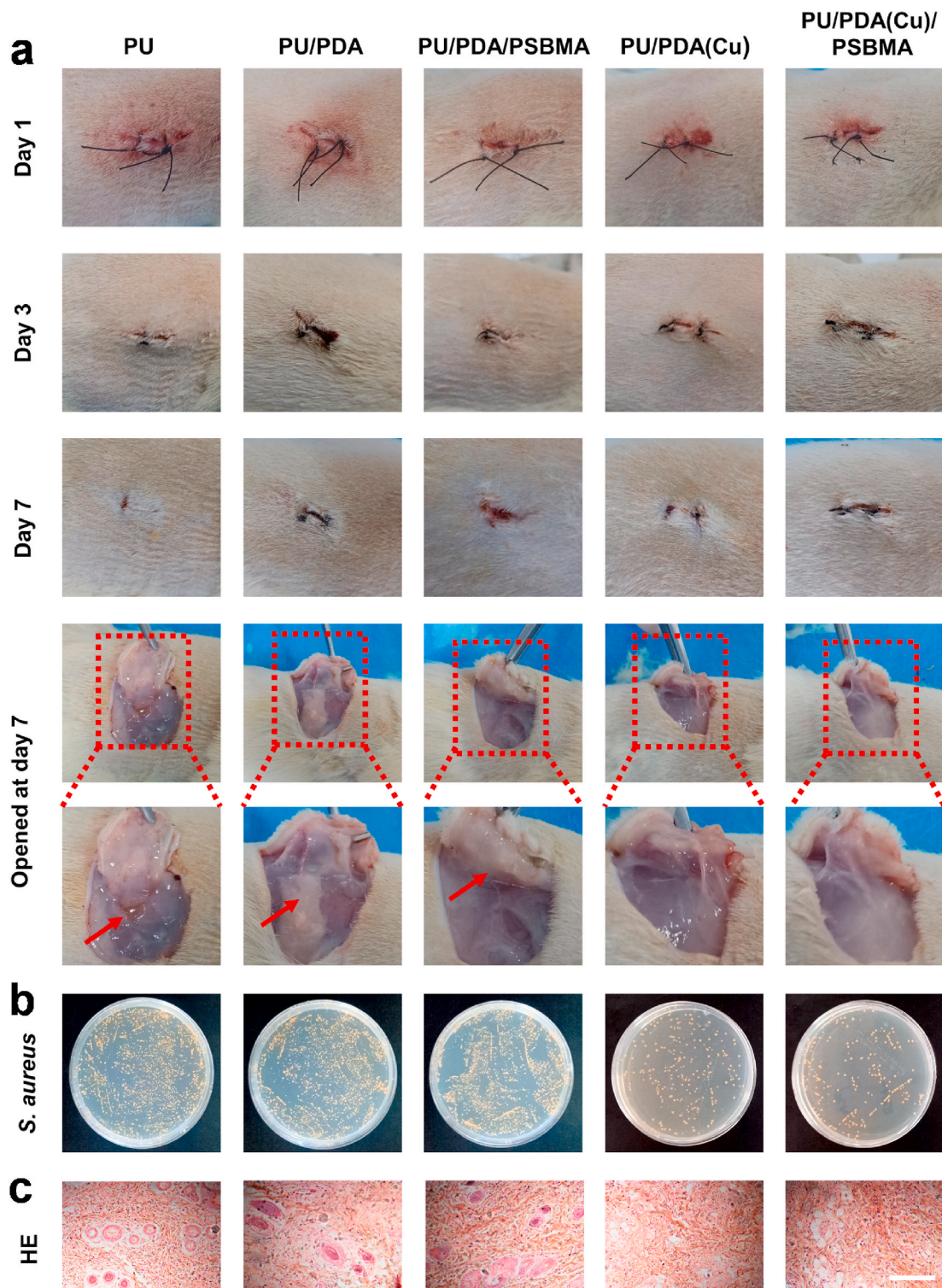
Fig. 7. (a) The photographs of PU, PU/PDA, PU/PDA/PSBMA, PU/PDA(Cu) and PU/PDA(Cu)/PSBMA implanted with mice infected with *S. aureus* (the red arrows indicated the pus). (b) LB agar plates of *S. aureus* number in pus upon treatment with PU, PU/PDA, PU/PDA/PSBMA, PU/PDA(Cu) and PU/PDA(Cu)/PSBMA, respectively. (c) HE staining of the surrounding connective tissues upon treatment with PU, PU/PDA, PU/PDA/PSBMA, PU/PDA(Cu) and PU/PDA(Cu)/PSBMA, respectively., respectively. Scale bar: 50 μm.

manuscript. Ziyue Long, Jiefang Wang and Yifan Ge did surface feature testing. Chengbo Cao, Hao Chen, Qiang Gao completed animal experiment part and revised the manuscript. Yongchun Meng and Bailiang Wang designed the work and revised the manuscript.

Declaration of competing interest

There are no conflicts to declare.

Acknowledgments

This work was supported by the National Natural Science Foundation of China (31771026, 82072077), Zhejiang Provincial Natural Science Foundation of China (LR19H180001), Project of State Key Laboratory of Ophthalmology, Optometry and Visual Science, Wenzhou Medical University (J02-20190203), Wenzhou key program of scientific and technological innovation (ZY2019017), Natural Science Foundation of Shandong Province of China (NO. ZR2016CQ16) and Science and Technology Development Plan of Shandong Province of China (2020YD096) which are greatly acknowledged.

Appendix A. Supplementary data

Supplementary data to this article can be found online at https://doi.org/10.1016/j.bioactmat.2021.01.025.

References

[1] S. Noimark, C.W. Dunnill, M. Wilson, I.P. Parkin, The role of surfaces in catheter-associated infections, Chem. Soc. Rev. 38 (12) (2009) 3435–3448.

[2] C.R. Arciola, D. Campoccia, L. Montanaro, Implant infections: adhesion, biofilm formation and immune evasion, Nat. Rev. Microbiol. 16 (7) (2018) 397–409.

[3] J.-J. Parienti, N. Mongardon, B. Megarbane, J.-P. Mira, P. Kalfon, A. Gros, S. Marque, M. Thuong, V. Pottier, M. Ramakers, B. Savary, A. Seguin, X. Valette, N. Terzi, B. Sauneuf, V. Cattoir, L.A. Mermel, D. du Cheyron, S.S. Grp, Intravascular complications of central venous catheterization by insertion site, N. Engl. J. Med. 373 (13) (2015) 1220–1229.

[4] R. Gbyli, A. Mercaldi, H. Sundaram, K.A. Amoako, Achieving totally local anticoagulation on blood contacting devices, Advanced Materials Interfaces 5 (4) (2018) 1700954.

[5] M.B. Gorbet, M.V. Sefton, Biomaterial-associated thrombosis: roles of coagulation factors, complement, platelets and leukocytes, Biomaterials 25 (26) (2004) 5681–5703.

[6] H.-C. Flemming, J. Wingender, U. Szewzyk, P. Steinberg, S.A. Rice, S. Kjelleberg, Biofilms: an emergent form of bacterial Life, Nat. Rev. Microbiol. 14 (9) (2016) 563–575.

[7] D. Davies, Understanding biofilm resistance to antibacterial agents, Nat. Rev. Drug Discov. 2 (2) (2003) 114–122.

[8] X. Laloyaux, E. Fautre, T. Blin, V. Purohit, J. Leprince, T. Jouenne, A.M. Jonas, K. Glinel, Temperature-responsive polymer brushes switching from bactericidal to cell-repellent, Adv. Mater. 22 (44) (2010) 5024–5028.

[9] X. Liu, L. Yuan, D. Li, Z. Tang, Y. Wang, G. Chen, H. Chen, J.L. Brash, Blood compatible materials: state of the art, J. Mater. Chem. B 2 (35) (2014) 5718–5738.

[10] S. Schwarz, A. Loeffler, K. Kadlec, Bacterial resistance to antimicrobial agents and its impact on veterinary and human medicine, Vet. Dermatol. 28 (1) (2017), 82-e19.

[11] R.A. Hoshi, R. Van Lith, M.C. Jen, J.B. Allen, K.A. Lapidos, G. Ameer, The blood and vascular cell compatibility of heparin-modified ePTFE vascular grafts, Biomaterials 34 (1) (2013) 30–41.

[12] Q. Xu, X. Li, Y. Jin, L. Sun, X. Ding, L. Liang, L. Wang, K. Nan, J. Ji, H. Chen, B. Wang, Bacterial self-defense antibiotics release from organic-inorganic hybrid multilayer films for long-term anti-adhesion and biofilm inhibition properties, Nanoscale 9 (48) (2017) 19245–19254.

[13] B. Furie, B.C. Furie, Mechanisms of disease: mechanisms of thrombus formation, N. Engl. J. Med. 359 (9) (2008) 938–949.

[14] I. Banerjee, R.C. Pangule, R.S. Kane, Antifouling coatings: recent developments in the design of surfaces that prevent fouling by proteins, bacteria, and marine organisms, Adv. Mater. 23 (6) (2011) 690–718.

[15] J. Jiang, L. Zhu, L. Zhu, H. Zhang, B. Zhu, Y. Xu, Antifouling and antimicrobial polymer membranes based on bioinspired polydopamine and strong hydrogen-bonded poly(N-vinyl pyrrolidone), ACS Appl. Mater. Interfaces 5 (24) (2013) 12895–12904.

[16] M. Zhang, Q.T. Nguyen, Z. Ping, Hydrophilic modification of poly (vinylidene fluoride) microporous membrane, J. Membr. Sci. 327 (1–2) (2009) 78–86.

[17] Y. Yang, P. Qi, F. Wen, X. Li, Q. Xia, M.F. Maitz, Z. Yang, R. Shen, Q. Tu, N. Huang, Mussel-inspired one-step adherent coating rich in amine groups for covalent immobilization of heparin: hemocompatibility, growth behaviors of vascular cells, and tissue response, ACS Appl. Mater. Interfaces 6 (16) (2014) 14608–14620.

[18] Z. Yang, J. Wang, R. Luo, M.F. Maitz, F. Jing, H. Sun, N. Huang, The covalent immobilization of heparin to pulsed-plasma polymeric allylamine films on 316L stainless steel and the resulting effects on hemocompatibility, Biomaterials 31 (8) (2010) 2072–2083.

[19] G. Cheng, G. Li, H. Xue, S. Chen, J.D. Bryers, S. Jiang, Zwitterionic carboxybetaine polymer surfaces and their resistance to long-term biofilm formation, Biomaterials 30 (28) (2009) 5234–5240.

[20] R.S. Smith, Z. Zhang, M. Bouchard, J. Li, H.S. Lapp, G.R. Brotske, D.L. Lucchino, D. Weaver, L.A. Roth, A. Coury, J. Biggerstaff, S. Sukavaneshvar, R. Langer, C. Loose, Vascular catheters with a nonleaching poly-sulfobetaine surface modification reduce thrombus formation and microbial attachment, Sci. Transl. Med. 4 (153) (2012) 153ra132.

[21] J.B. Schlenoff, Zwitteration: coating surfaces with zwitterionic functionality to reduce nonspecific adsorption, Langmuir 30 (32) (2014) 9625–9636.

[22] A.J. Keefe, S. Jiang, Poly(zwitterionic)protein conjugates offer increased stability without sacrificing binding affinity or bioactivity, Nat. Chem. 4 (1) (2012) 60–64.

[23] P.J. Molino, D. Yang, M. Penna, K. Miyazawa, B.R. Knowles, S. MacLaughlin, T. Fukuma, I. Yarovsky, M.J. Higgins, Hydration layer structure of biofouling-resistant nanoparticles, ACS Nano 12 (11) (2018) 11610–11624.

[24] C. Leng, H.-C. Hung, S. Sun, D. Wang, Y. Li, S. Jiang, Z. Chen, Probing the surface hydration of nonfouling zwitterionic and PEG materials in contact with proteins, ACS Appl. Mater. Interfaces 7 (30) (2015) 16881–16888.

[25] H. Chen, J. Yang, L. Sun, H. Zhang, Y. Guo, J. Qu, W. Jiang, W. Chen, J. Ji, Y.-W. Yang, B. Wang, Synergistic chemotherapy and photodynamic therapy of endophthalmitis mediated by zeolitic imidazolate framework-based drug delivery systems, Small 15 (47) (2019) 1903880.

[26] X. Ding, S. Duan, X. Ding, R. Liu, F.-J. Xu, Versatile antibacterial materials: an emerging arsenal for combatting bacterial pathogens, Adv. Funct. Mater. 28 (40) (2018) 1802140.

[27] J. He, Y. Qiao, H. Zhang, J. Zhao, W. Li, T. Xie, D. Zhong, Q. Wei, S. Hua, Y. Yu, K. Yao, H.A. Santos, M. Zhou, Gold silver nanoshells promote wound healing from drug-resistant dacteria infection and enable monitoring via surface-enhanced Raman scattering imaging, Biomaterials 234 (2020) 119763.

[28] Z. Li, D. Lee, X. Sheng, R.E. Cohen, M.F. Rubner, Two-level antibacterial coating with both release-killing and contact-killing capabilities, Langmuir 22 (24) (2006) 9820–9823.

[29] S. Chernousova, M. Epple, Silver as antibacterial agent: ion, nanoparticle, and metal, Angew. Chem. Int. Ed. 52 (6) (2013) 1636–1653.

[30] Y. Jiao, L.-N. Niu, S. Ma, J. Li, F.R. Tay, J.-H. Chen, Quaternary ammonium-based biomedical materials: state-of-the-art, toxicological aspects and antimicrobial resistance, Prog. Polym. Sci. 71 (2017) 53–90.

[31] N.M.O. Andoy, K. Jeon, C.T. Kreis, R.M.A. Sullan, Multifunctional and stimuli-responsive polydopamine nanoparticle-based platform for targeted antimicrobial applications, Adv. Funct. Mater. 30 (40) (2020) 2004503.

[32] R. Trammell, K. Rajabimoghadam, I. Garcia-Bosch, Copper-promoted functionalization of organic molecules: from biologically relevant Cu/O-2 model systems to organometallic transformations, Chem. Rev. 119 (4) (2019) 2954–3031.

[33] L.-S. Lin, T. Huang, J. Song, X.-Y. Ou, Z. Wang, H. Deng, R. Tian, Y. Liu, J.-F. Wang, Y. Liu, G. Yu, Z. Zhou, S. Wang, G. Niu, H.-H. Yang, X. Chen, Synthesis of copper peroxide nanodots for H_2O_2 self-supplying chemodynamic therapy, J. Am. Chem. Soc. 141 (25) (2019) 9937–9945.

[34] M.E. Douglass, M.J. Goudie, J. Pant, P. Singha, S. Hopkins, R. Devine, C.W. Schmiedt, H. Handa, Catalyzed nitric oxide release via Cu nanoparticles leads to an increase in antimicrobial effects and hemocompatibility for short-term extracorporeal circulation, ACS Appl. Bio. Mater. 2 (6) (2019) 2539–2548.

[35] K.K. Konopinska, N.J. Schmidt, A.P. Hunt, N. Lehnert, J. Wu, C. Xi, M.E. Meyerhoff, Comparison of copper(II)-Ligand complexes as mediators for preparing electrochemically modulated nitric oxide-releasing catheters, ACS Appl. Mater. Interfaces 10 (30) (2018) 25047–25055.

[36] C.W. McCarthy, R.J. Guillory 2nd, J. Goldman, M.C. Frost, Transition-metal-mediated release of nitric oxide (NO) from S-nitroso-N-acetyl-d-penicillamine (SNAP): potential applications for endogenous release of NO at the surface of stents via corrosion products, ACS Appl. Mater. Interfaces 8 (16) (2016) 10128–10135.

[37] J. Pant, J. Gao, M.J. Goudie, S.P. Hopkins, J. Locklin, H. Handa, A multi-defense strategy: enhancing bactericidal activity of a medical grade polymer with a nitric oxide donor and surface-immobilized quaternary ammonium compound, Acta Biomater. 58 (2017) 421–431.

[38] J. Pant, M.J. Goudie, S.M. Chaji, B.W. Johnson, H. Handa, Nitric oxide releasing vascular catheters for eradicating bacterial infection, J. Biomed. Mater. Res. B Appl. Biomater. 106 (8) (2018) 2849–2857.

[39] J. Pant, M.J. Goudie, S.P. Hopkins, E.J. Brisbois, H. Handa, Tunable nitric oxide release from S-nitroso-N-acetylpenicillamine via catalytic copper nanoparticles for biomedical applications, ACS Appl. Mater. Interfaces 9 (18) (2017) 15254–15264.

[40] H. Lee, S.M. Dellatore, W.M. Miller, P.B. Messersmith, Mussel-inspired surface chemistry for multifunctional coatings, Science 318 (5849) (2007) 426–430.

[41] X. Du, L. Li, J. Li, C. Yang, N. Frenkel, A. Welle, S. Heissler, A. Nefedov, M. Grunze, P.A. Levkin, UV-triggered dopamine polymerization: control of polymerization, surface coating, and photopatterning, Adv. Mater. 26 (47) (2014) 8029–8033.

[42] C. Zhang, H.-N. Li, Y. Du, M.-Q. Ma, Z.-K. Xu, $CuSO_4/H_2O_2$-Triggered polydopamine/poly(sulfobetaine methacrylate) coatings for antifouling membrane surfaces, Langmuir 33 (5) (2017) 1210–1216.

[43] C. Zhang, Y. Ou, W.-X. Lei, L.-S. Wan, J. Ji, Z.-K. Xu, $CuSO_4/H_2O_2$-Induced rapid deposition of polydopamine coatings with high uniformity and enhanced stability, Angew. Chem. Int. Ed. 55 (9) (2016) 3054–3057.

[44] H. Ejima, J.J. Richardson, F. Caruso, Metal-phenolic networks as a versatile platform to engineer nanomaterials and biointerfaces, Nano Today 12 (2017) 136–148.

[45] Q. Tu, X. Shen, Y. Liu, Q. Zhang, X. Zhao, M.F. Maitz, T. Liu, H. Qiu, J. Wang, N. Huang, Z. Yang, A facile metal-phenolic-amine strategy for dual-functionalization of blood-contacting devices with antibacterial and anticoagulant properties, Mater. Chem. Front. 3 (2) (2019) 265–275.

[46] Z. Yang, Y. Yang, K. Xiong, J. Wang, H. Lee, N. Huang, Metal-phenolic surfaces for generating therapeutic nitric oxide gas, Chem. Mater. 30 (15) (2018) 5220–5226.

[47] E.J. Brisbois, R.P. Davis, A.M. Jones, T.C. Major, R.H. Bartlett, M.E. Meyerhoff, H. Handa, Reduction in thrombosis and bacterial adhesion with 7 Day implantation

of S-nitroso-N-acetylpenicillamine (SNAP)-Doped elast-eon E2As catheters in sheep, J. Mater. Chem. B 3 (8) (2015) 1639–1645.

[48] X. Li, P. Gao, J. Tan, K. Xiong, M.F. Maitz, C. Pan, H. Wu, Y. Chen, Z. Yang, N. Huang, Assembly of metal phenolic/catecholamine networks for synergistically anti-inflammatory, antimicrobial, and anticoagulant coatings, ACS Appl. Mater. Interfaces 10 (47) (2018) 40844–40853.

[49] T. Feng, W. Ji, Y. Zhang, F. Wu, Q. Tang, H. Wei, L. Mao, M. Zhang, Zwitterionic polydopamine engineered interface for in vivo sensing with high biocompatibility, Angew. Chem. Int. Ed. 59 (2020) 1–6.

[50] H. Ejima, J.J. Richardson, K. Liang, J.P. Best, M.P. van Koeverden, G.K. Such, J. Cui, F. Caruso, One-step assembly of coordination complexes for versatile film and particle engineering, Science 341 (6142) (2013) 154–157.

[51] G. Liu, K. Li, H. Wang, L. Ma, L. Yu, Y. Nie, Stable fabrication of zwitterionic coating based on copper-phenolic networks on contact lens with improved surface wettability and broad-spectrum antimicrobial activity, ACS Appl. Mater. Interfaces 12 (14) (2020) 16125–16136.

[52] X. Chen, H. Gu, Z. Lyu, X. Liu, L. Wang, H. Chen, J.L. Brash, Sulfonate groups and saccharides as essential structural elements in heparin-mimicking polymers used as surface modifiers: optimization of relative contents for antithrombogenic properties, ACS Appl. Mater. Interfaces 10 (1) (2018) 1440–1449.

[53] W.S. Choi, Y.K. Joung, Y. Lee, J.W. Bae, H.K. Park, Y.H. Park, J.-C. Park, K.D. Park, Enhanced patency and endothelialization of small-caliber vascular grafts fabricated by coimmobilization of heparin and cell-adhesive peptides, ACS Appl. Mater. Interfaces 8 (7) (2016) 4336–4346.

[54] N. Mackman, Triggers, targets and treatments for thrombosis, Nature 451 (7181) (2008) 914–918.

[55] I.H. Jaffer, J.C. Fredenburgh, J. Hirsh, J.I. Weitz, Medical device-induced thrombosis: what causes it and how can we prevent it? J. Thromb. Haemostasis 13 (2015) S72–S81.

[56] D. Hu, L. Zou, Y. Gao, Q. Jin, J. Ji, Emerging nanobiomaterials against bacterial infections in postantibiotic era, View 1 (3) (2020) 20200014.

[57] P.P. Pillai, B. Kowalczyk, K. Kandere-Grzybowska, M. Borkowska, B. A. Grzybowski, Engineering Gram selectivity of mixed-charge gold nanoparticles by tuning the balance of surface charges, Angew. Chem. Int. Ed. 55 (30) (2016) 8610–8614.

[58] X. Zhang, X. Chen, J. Yang, H.-R. Jia, Y.-H. Li, Z. Chen, F.-G. Wu, Quaternized silicon nanoparticles with polarity-sensitive fluorescence for selectively imaging and killing gram-positive bacteria, Adv. Funct. Mater. 26 (33) (2016) 5958–5970.